KSME International Journal, Vol. 13, No. 8, pp. 585~594, 1999

Experimental Modal Analysis on the Core Support Barrel of Reactor Internals Using a Scale Model

Seon Ho Song* and Myung Jo Jhung*

(Received December 9, 1998)

The vibration of core support barrel (CSB) in a typical pressurized water reactor is studied by experimental and finite element analysis methods. Free vibration models are built and tested for the 1/13.7th scale of Ulchin Nuclear (UCN) Unit 3 & 4. Finite element model is established by plate model with shell elements. Finite element and measurement analyses are performed with respect to the two type of cylindrical shell models with and without holes. Test results on CSB vibration models are presented and compared with finite element analysis results. Various techniques are used to compare the measurement and analysis results.

Key Words: Core Support Barrel, Modal Analysis, Correlation, Mode Shape, Frequency Response Function

1. Introduction

During normal operations of a nuclear power plant, the core support barrel moves with infinitesimally small amplitudes by the random thermo-hydraulic load of reactor coolant flow. Flow-induced vibration of reactor internals has been investigated extensively to assure the reliability of CSB and to obtain information that will enable a designer to predict plant vibration amplitudes for improved design (ANSI and ASME, 1994).

The Ulchin Nuclear Unit 3 & 4, which is of new structural design, has not been confirmed that the CSB is adequately dimensioned for the operational vibration loads during the service life of the reactor. A Comprehensive Vibration Assessment Program was carried out recently to determine the flow-induced vibration of the Yonggwang Nuclear Unit 4 internals over wide ranges of flow and temperature (Kim et al., 1995). It was required by the Regulatory Guide 1. 20 of US Nuclear Regulatory Commission (USNRC, 1976).

Much valuable information on the dynamics of reactor internals can be obtained from model tests. This includes the excitation mechanisms, the corresponding vibration responses, the mechanical impedances of the internals, and the characteristics of the system damping. Because of the requirements on geometric, kinematic, and dynamic similarity, reactor models are quite expensive and difficult to construct and to test. To obtain satisfactory results, elaborate techniques of model construction and test instrumentation have been developed at the NSSS system manufacturer during the past years (Lee, 1974; Jhung, 1992).

The purpose of this paper is to conform the adequate modal analysis technique for describing the CSB motion of UCN Unit 3 & 4 using a scale model. Free vibration models are built and tested for the 1/13. 7th scale model. Test results on CSB vibration models are presented and compared with finite element analysis results. Various modal analysis techniques are used to show agreement between the measurement and analysis results. By utilizing scaled test results, the flow induced vibration of the actual reactor internals can be predicted.

* Mechanical Engineering Department, Korea Institute of Nuclear Safety, 19 Kusong-dong, Yusong-gu, Taejon 305-338, Korea

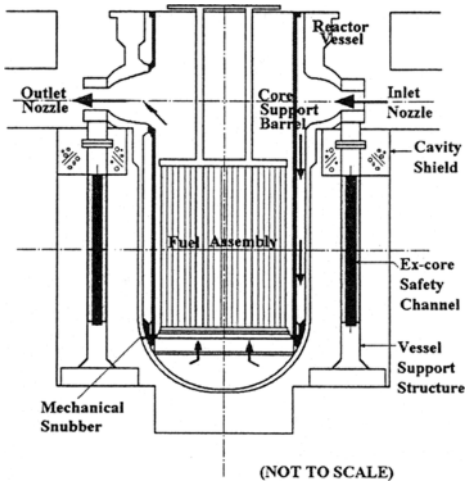

Fig. 1 Cross sectional view of reactor arrangement.

Table 1 Principal dimensions of 1/13. 7th scale CSB model

Items	CSB of UCN [mm]	1/13.7 Scale Model [mm]
Out Diameter	3657.6	267.0
Thickness	76.2	5.5
Length of CSB	9620.3	700.0
Inlet Nozzle ID	1184.3	86.0
Nozzle Distance from CSB flange	3564.0	260. 0

2. Experiment

2.1 Description of vibration model

Fig. 1 shows a cross sectional view of a typical pressurized water reactor vessel and a core support barrel. The principal dimensions of the CSB vibration model are exactly 1/13.7th as large as the corresponding dimensions of the UCN Unit 3 & 4 CSB, as shown in Table 1.

The geometry of the CSB can be changed with relative ease and at low cost. Schematic view of the test model is shown in Fig. 2. The major difference between the test model and the prototype CSB is that the model does not have flow inner and outer surfaces of CSB. The fluid effect will be included by increasing the mass of the structure when results from in-air and in-water conditions are available (Jhung, 1996).

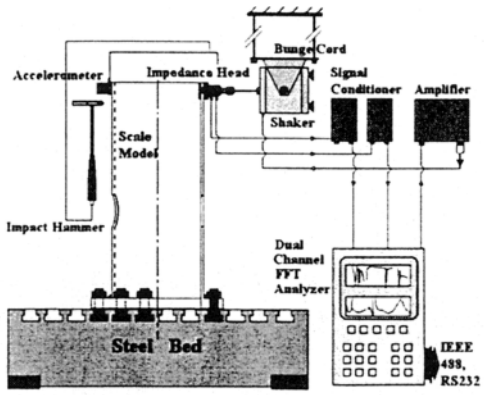

Fig. 2 Schematic views of the test model.

2.2 Model test and data acquisition methods

The natural frequencies and mode shapes of the CSB model were measured in air with the instrumentation shown in Fig. 2. Impact hammer test was performed to obtain improved understanding of the vibration modes of CSB and to determine how well the natural frequencies and the mode shapes of the simplified CSB model agree with the finite element analysis results obtained from ANSYS (ANSYS, 1996).

For the in-air test, the CSB model was placed on the work bench upside down, as shown in Fig. 2. The snubber of CSB was omitted in this test to provide a clamped-free boundary condition.

After completion of all measurements, the frequency response function (FRF) of inertance data were transferred in the form of . FRF files (ICATS, 1998). This was achieved using analyzer interface program that could produce Type 58 universal files. A typical measured FRF, phase and modulus, of the CSB model is shown in Fig. 3, where the regenerated FRF data is also shown and there is an excellent agreement between them.

Before undertaking a modal analysis, a combined response data file was created by using the ICATS software (ICATS, 1998). This file contains the names of the individual.FRF files, their number and the position of the point measurement, i. e. the particular FRF measurement for which the excitation and response points are coincident. This is particularly important as the mass-normalization of the mode shape vectors requires this information.

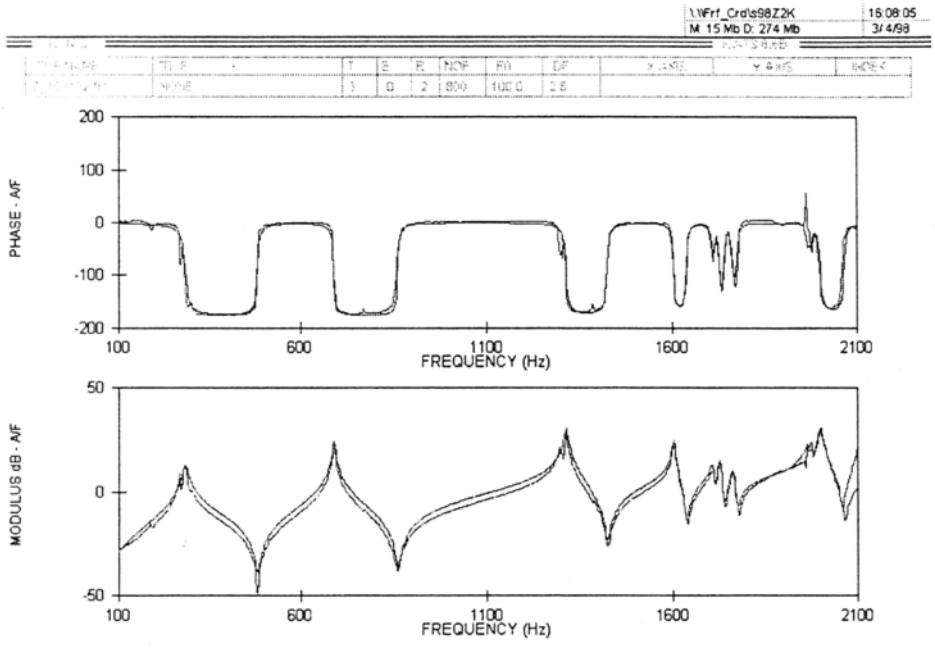

Fig. 3 Typical measured FRF, phase and modulus of the CSB model.

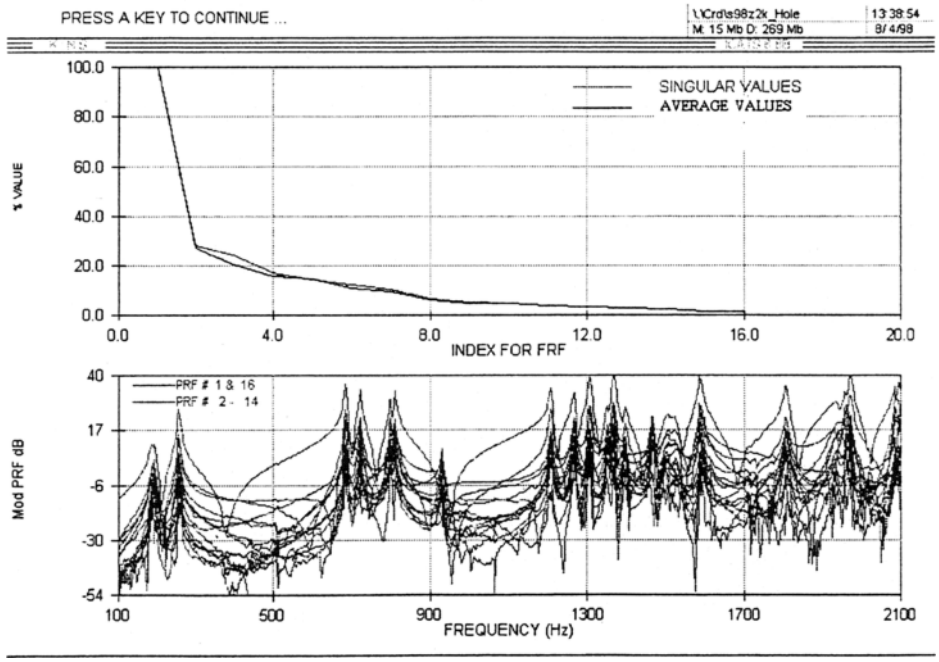

Fig. 4 Principal response function analysis.

Using the Principal Response Function approach, the quality of the measured FRF data was checked. All 20 FRF files are plotted together on the lower display of Fig. 4.

The singular values, together with the averaged FRF values, are shown on the upper display. It is

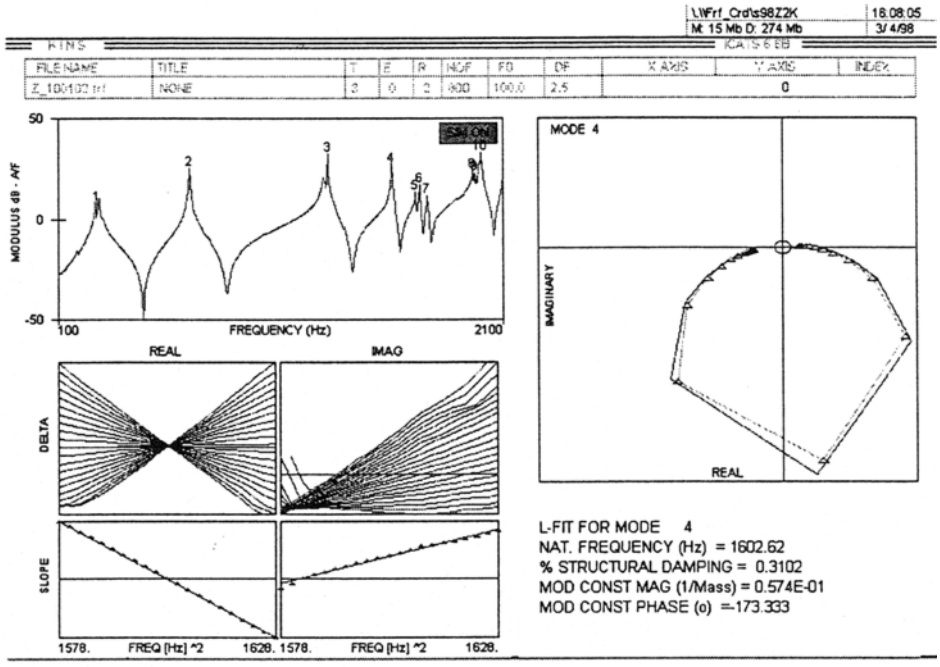

Fig. 5 Line-fit analysis result.

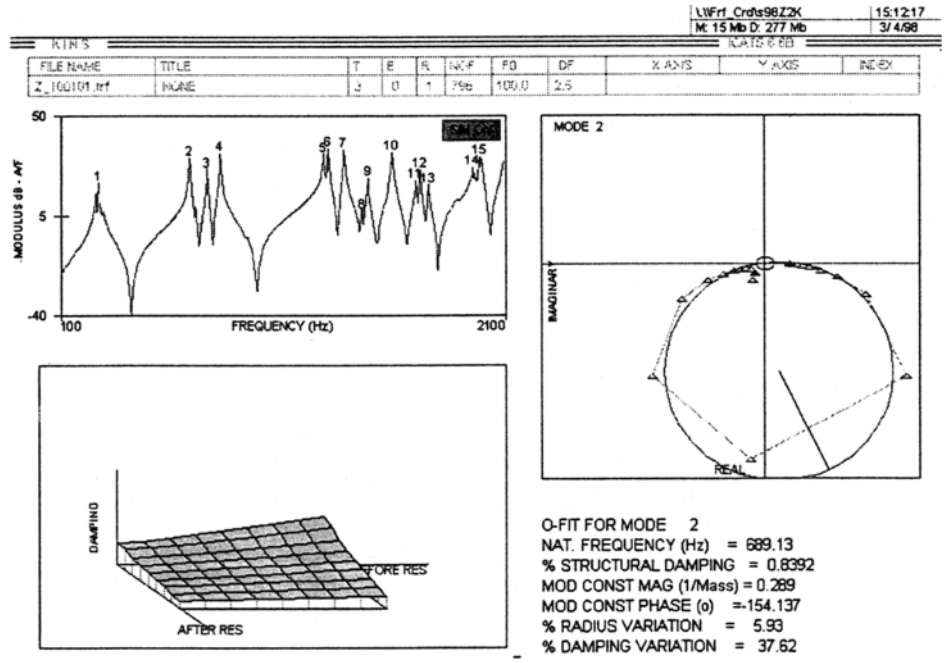

Fig. 6 Circle-fit analysis result.

easily seen that the number of non-zero singular values is about 16, indicating that there are 16 active modes in the range considered (100–2100 Hz)

Prior to analyzing the measured FRFs, the identical analysis was performed and the regener-

ated FRF was plotted over the experimental data (Fig. 3). Although the overall quality of the fit is acceptable, more improvements can be achieved by refining the experimental model via SDOF techniques.

Fig. 5 shows a line-fit analysis result where a least-squares line is fitted to the inverse of the FRF in the Argand plane. In this figure, four windows drawn in the bottom left-hand corner of the screen indicate the variation of the real and imaginary parts of the inverse FRF when viewed from all possible combinations found using all of the selected Nyquist points.

Fig. 6 shows the circle-fit analysis result where the classic SDOF analysis of fitting a circle is performed to a Nyquist plot around resonance. A 21-point Nyquist plot of a certain mode is displayed with 10 points on either side of the resonance. Figure 6 shows a very good agreement between the regenerated Nyquist and the original one, which indicates the analysis quality. A three -dimensional damping plot drawn in the bottom left-hand corner of the screen indicates the variation of the damping values with respect to different frequency points. It is shown from this figure that the consistency of the damping values is obtained by using circle fit analysis with all available FRF data points. The result is a matrix of damping values, the number of columns being determined by the number of data points before resonance, and the number of rows by the number of data points after resonance. As the damping plot is flat and the calculated damping value is an invariant with respect to FRF data used in this figure, the mode under consideration is concluded to be linear.

2.3 Collating individual FRF analysis

The individually analyzed FRFs exhibiting slightly different modal parameters were checked whether the collations are successful for those modes. Fig. 7 shows a matrix of modal parameter files against modes found in this experiment. The tolerance value 7% is given to distinguish between two separate modes. In this figure, 16 modes are identified. A white-grey grid box indicates that the corresponding mode was found in that particular FRF file while a black box indicates the opposite. Hence, a mode with a complete line of white-grey boxes has been identified in all FRFs and the collation is successful for that mode.

An alternative way of modal analysis technique, GLOBAL_M, was used to analyze all FRFs in one single sweep for modes for each frequency window considered. GLOBAL_M is based on a complex singular value decomposition of a system matrix expressed in terms of measured FRF properties and then on a complex eigensolution which extracts the required modal properties. Theoretically, a minimum of N FRFs are required to analyze N modes simultaneously. In this measurement, 40 nodal points were measured generating 40 FRFs. Fig. 8 shows the GLOBALM analysis result from 40 FRFs of the CSB model.

From the individually analyzed FRFs and the modal parameter files, eigen files were created to regenerate the FRFs, to order the coordinates and to animate the mode shapes. The mode shapes were mass-normalized using the point measure-

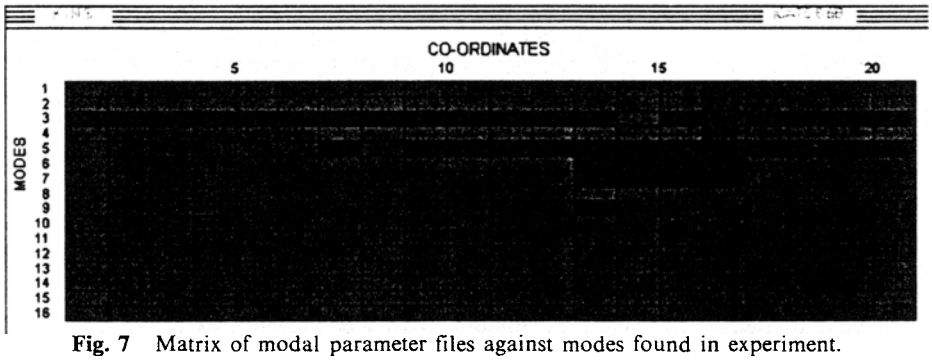

Fig. 7 Matrix of modal parameter files against modes found in experiment.

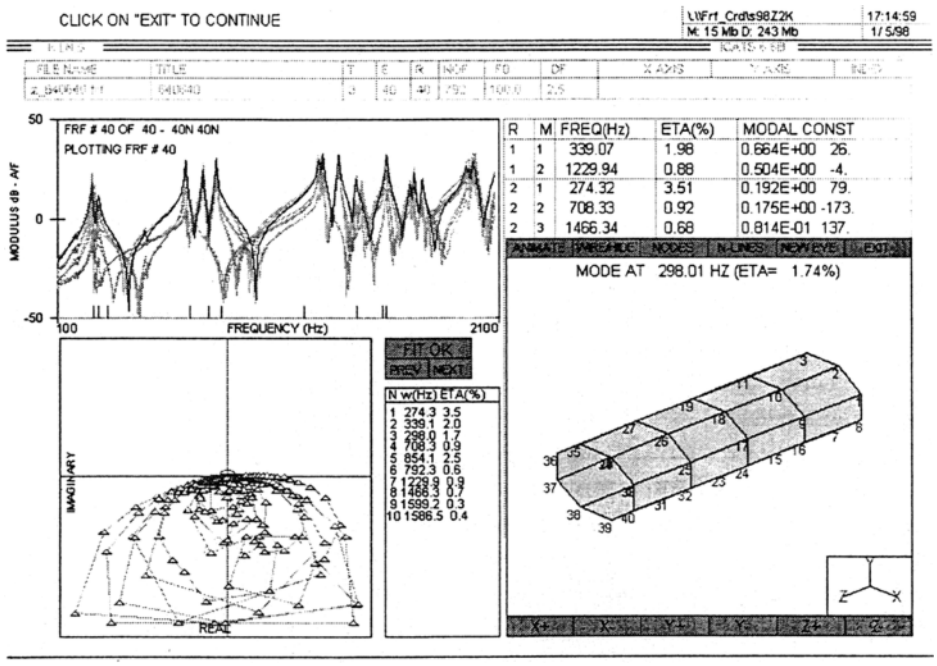

Fig. 8 GLOBAL_M analysis result.

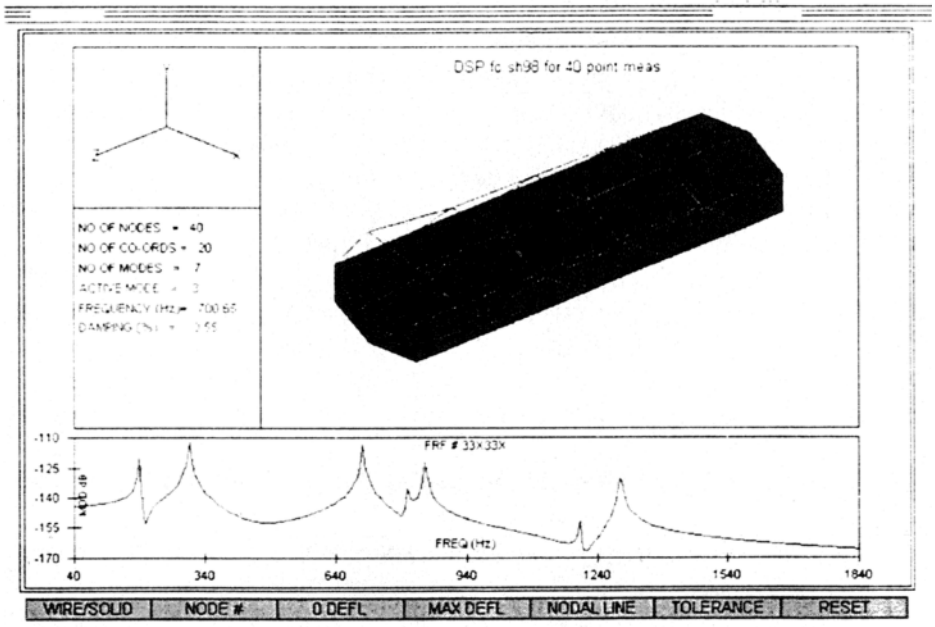

Fig. 9 Animated mode of the CSB test model.

ment information.

One of the mode shapes of CSB model was animated to assess whether it is physically plausible. To achieve this, a geometry file was created via MESHGEN in ICATS software. Figure 9 shows a animated mode of the CSB test model.

To assess the complexity of each mode (Ewins, 1995), the mode shape elements are plotted as

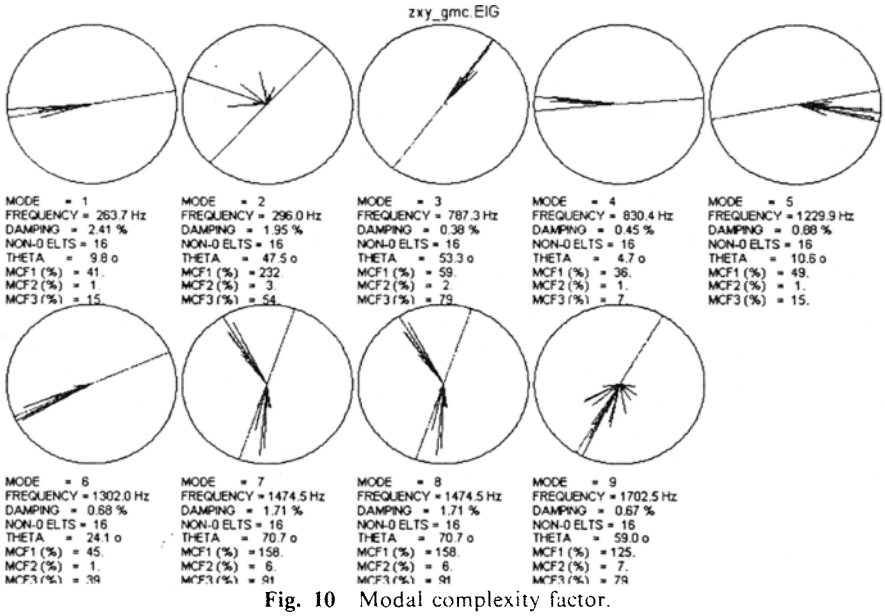

Fig. 10 Modal complexity factor.

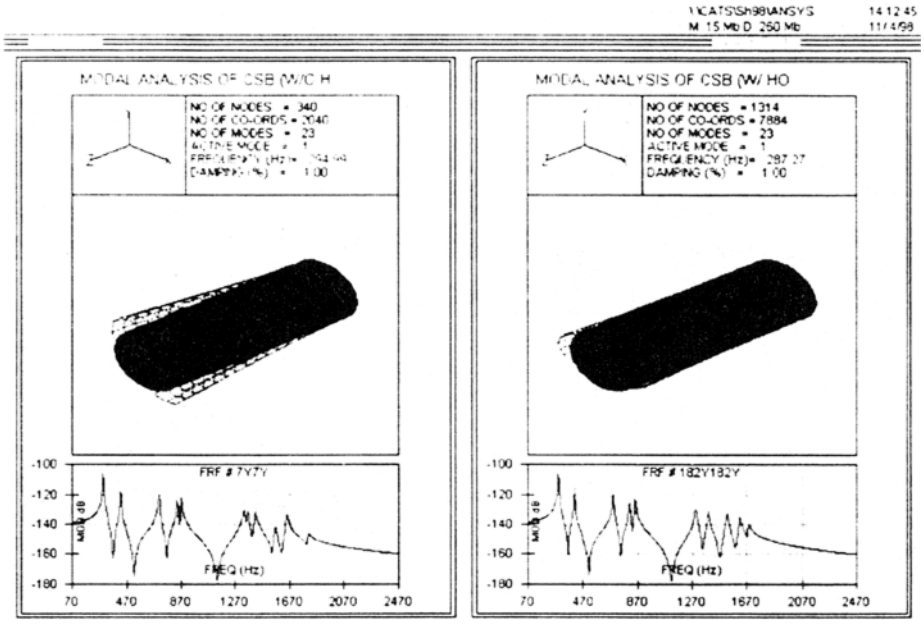

Fig. 11 FRFs and mode shapes obtained from the ANSYS finite element models.

vectors in Fig. 10, the length of each being the magnitude of the individual element, with the angle with the X axis representing its phase. The almost-real modes are those with vectors tending to form a straight line

2.4 Finite element model

The ANSYS finite element analysis program was used to model the CSB structure. Two finite element models were generated for the CSB scale models, i. e. with and without holes to see whether the holes affect the modal parameters of

the shell model. Axisymmetric harmonic structural shell (SHELL61) and Householder reduced method are used in the analysis for element and modal extraction method, respectively. The ANSYS eigensolutions corresponding to the model transferred from ANSYS into standard ICATS format. Fig. 11 shows the FRFs and mode shapes obtained from the ANSYS finite element models. Frequency comparisons between models with and without holes are shown in Table 2 and there is a good agreement between them with frequencies of less than 5% discrepancy. Therefore the hole effect on the modal characteristics is found to be negligible.

Table 2 Natural frequencies of shells with and without holes from finite element method analysis

Serial mode	Frequency (Hz)		Mode number	
	w/o hole	w/ hole	Axial	Circum.
1	295	288-290	1	2
2	424	401-403	1	1
3	704	693-693	1	3
4	839	831-833	2	2
5	869	856-857	2	3
6	1336	1325-1325	1	4
7	1361	1308-1354	3	3
8	1420	1405-1420	2	4
9	1578	1546-1560	2	1
10	1654	1634-1667	3	4
11	1812	1724-1828	3	2

3. Correlation Analysis

Measured and analyzed natural frequencies were compared with each other to see the correlation of the CSB model. Natural frequencies of the measured set (set 2) are now plotted against those of analyzed set (set 1) in upper left hand side of Fig. 12. A reference 45o line is also plotted for convenience. By detecting data points consistently lying both side of the reference line, it can be guessed that no systematic discrepancies exist in the CSB modal analysis.

A two-degree grid plot of the modal assurance criterion is displayed in upper right hand side of Fig. 12. The actual modal assurance criterion values can be retracted using the colour-code

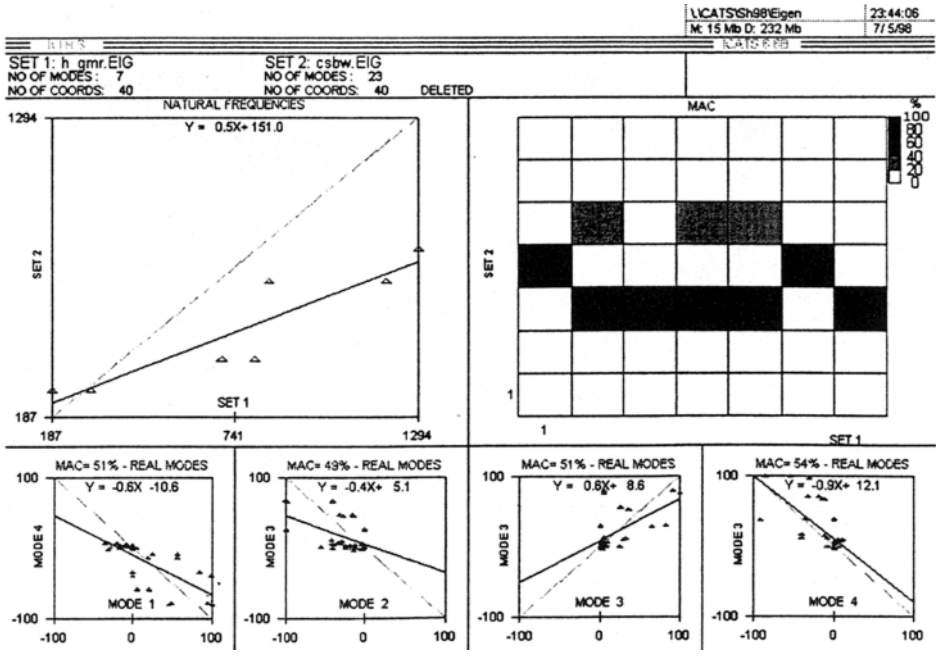

Fig. 12 Natural frequency, modal assurance criterion and mode shape comparisons.

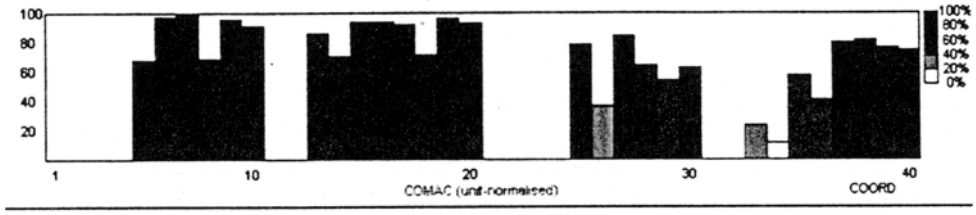

Fig. 13 Coordinate assurance criterion and mode shape comparisons.

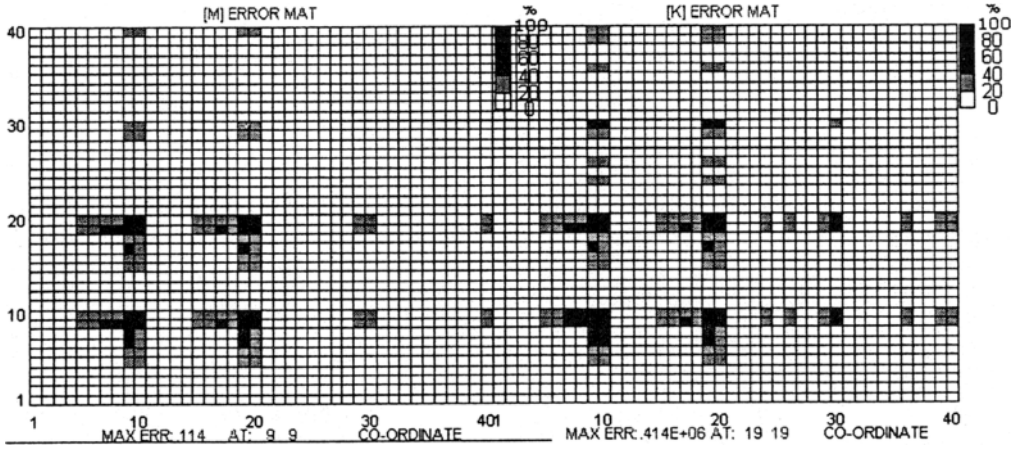

Fig. 14 Mass and stiffness error matrices.

given in the right hand side. Ideally, the modal assurance criterion plot should clearly exhibit a 45° line, indicating an ordered correlation of modes from measured and analyzed data set.

Modes up to 7 show some degree of one-to-one correlation. However, there are problems with most of the higher modes. The low modal assurance criterion values of 50% shows that the mode has been identified alone by either the finite element model or the experimental model.

The mode shape pairs identified by the modal assurance criterion plot are plotted against each other for further comparison. In the bottom side of Fig. 12, closely correlated mode shapes produce points that lie on a positive or negative 45° line. This reference line and the least-squares equation of the actual plot are also displayed for convenience.

Relatively well-correlated mode pairs are selected to see the coordinate modal assurance criterion. A bar-graph indicating the degree of correlation for each coordinate is displayed in Fig. 13. Low value of the coordinate modal assurance criterion is an indication of poor correlation at these coordinates in spite of the general agreement of the mode shape.

The stiffness error matrix is defined as $[E]=[K]_{FE}-[K]_{EXP}$, where $[K]_{EXP}$ is computed in terms of the identified modal data. The discrepancies between the finite element and measured analysis models are spotted using error matrix techniques in Figure 14. In this CSB model case, the correlated mode pairs (3 in total) was used for calculating the mass and stiffness error matrices. The maximum values for each matrix are displayed in this figure : 9 for the mass error matrix and 19 for the stiffness error matrix. The finite element analysis and measurement coordinates associated with this numbers should be given a close inspection.

4. Conclusions

Free vibration models are built and tested for the 1/13.7th scale of UCN 3 & 4 CSB. Finite element and measurement analyses are performed

with respect to the two shell models, one is shell with holes and the other is without hole. Test results on CSB vibration models are presented and compared with finite element analysis results. Various modal analysis techniques are used to show the agreement of measurement and analysis results.

On the basis of the investigations described in this study, the conclusions are as follows:

(1) The 1/13.7th scale model can predict the dynamic behavior of the actual core support barrel structure.

(2) A fine tuning technique and a more accurate finite element model should be constructed to guarantee precise agreement between the natural frequencies and mode shapes of the one identified by measurement and the one by the finite element analysis.

(3) The frequency response functions measured on the scale model are quite similar to those calculated on the finite element model.

(4) The existence of shell holes on the finite element model has little effects on the analysis results. In case of the measurement, however, the effects of shell hole on the modal frequencies and mode shapes are much larger than those of the shell without holes.

References

ANSI and ASME, 1994, "Inservice Monitoring of Core Support Barrel Axial Preload in Pressurized Water Reactors," ASME OM-S/G-1994 Guide Part 5. pp. 187~219.

ANSYS, 1996, *ANSYS Structural Analysis Guide*, ANSYS, Inc., Houston.

ICATS, 1998, "Modent, Modesh, Modacq, Meshgen Reference Manual," Imperial College, Mechanical Engineering Department.

Ewins, D. J., 1995, *Modal Testing: Theory and Practice*, 2nd ed., Research Studies Press, London.

Jhung, M. J., 1992, "Dynamic Characteristics of Reactor Core for Pipe Break and Seismic Excitations," *KSME Journal*, Vol. 6, No. 2, pp. 101~108.

Jhung, M. J., 1996, "Shell Response of Core Barrel for Tributary Pipe Break," *The International Journal of Pressure Vessels and Piping*, Vol. 69, No. 2, pp. 175~183.

Kim, Y. B. et al., 1995, "Assessment on Integrity of Reactor Internals Subjected to Fluid Induced Vibration," *Proc. '95 KSME Dynamics and Control Conference*, 95DC18, pp. 122~127.

Lee, H., 1974, "Prediction of the Flow-Induced Vibration of Reactor Internals by Scale Model Tests," WCAP-8317, Westinghouse Electric Corporation.

USNRC, 1976, "Comprehensive Vibration Assessment Program for Reactor Internals During Preoperational and Initial Startup Testing," Regulatory Guide 1. 20, US Nuclear Regulatory Commission.